A new specimen of *Sinopterus dongi* (Pterosauria, Tapejaridae) from the Jiufotang Formation (Early Cretaceous, China)

Caizhi Shen[1†], Rodrigo V. Pêgas[2†], Chualing Gao[1], Martin Kundrát[3], Lijun Zhang[4], Xuefang Wei[5], Xuanyu Zhou[6,7,8*]

1. Dalian Natural History Museum, Dalian, Liaoning, China.
2. Federal University of ABC, São Bernardo, Brazil.
3. Evolutionary Biodiversity Research Group, PaleoBioImaging Lab, Center for Interdisciplinary Biosciences, Technology and Innovation Park, Pavol Jozef Safárik University, Kosice, Slovak Republic.
4. Hainan Tropical Ocean University, Sanya, Hainan, China.
5. Institute of Geology, Chinese Academy of Geological Sciences, Beijing, China.
6. School of Sciences, Hokkaido University, Sapporo, Japan.
7. Hokkaido University Museum, Hokkaido University, Sapporo, Japan.
8. Beipiao Pterosaur Museum of China, Beipiao, Liaoning, China.

Corresponding Author:
Xuanyu Zhou
Hokkaido University, Sapporo, Japan
Email address: xyzhou@elms.hokudai.ac.jp

[†]These authors contributed equally to this work

Abstract

The Tapejarinae are edentulous pterosaurs that are relatively common in Cretaceous continental deposits in South America, North Africa, Europe, and China (mostly Early Cretaceous). The Chinese Jiufotang Formation is particularly rich in tapejarine specimens, having yielded over 10 described specimens and dozens of undescribed ones. For the Jiufotang Formation, a total of 7 nominal tapejarid species and 2 genera have been proposed. Some debate exists over how many

32 of those are valid or, alternatively, sexual or ontogenetic morphs of fewer (or even a single)

33 species. Despite the abundance of specimens and the relevant taxonomic problems involved,

34 detailed revisions of the matter are still lacking. This is partly due to the relatively scarce

35 knowledge on the comparative osteology of the *Sinopterus* complex, which is hampered by the

36 fact that most specimens have been only preliminarily described. In this contribution, we present

37 a new postcranial specimen, D3072, which we attribute to the type-species of the genus,

38 *Sinopterus dongi*. This new specimen helps shed some new light in the osteology of *Sinopterus*

39 *dongi*, hopefully serving as a basis for future comparative studies involving further specimens

40 and other proposed species and, subsequently, taxonomic revisions.

Introduction

43 The Tapejarinae (*sensu* Kellner & Campos, 2007) are a peculiar clade of Cretaceous edentulous

44 pterosaurs of the group Azhdarchoidea (Pterodactyloidea, Eupterodactyloidea), defined as the

45 most inclusive clade comprehending *Tapejara wellnhoferi* but not *Thalassodromeus sethi*

46 (Kellner & Campos, 2007). They are characterized by their short, downturned rostra and sagittal

47 premaxillary and dentary crests that start on the rostral region of the skull (Kellner & Campos,

48 2007). They comprise over 10 species (up to 19 proposed species), spanning from the Barremian

49 to the Santonian; with records from Brazil, Morocco, Europe and China (Kellner & Campos,

50 2007, Vullo *et al.*, 2012, Andres *et al.*, 2014, Pêgas *et al.*, 2016, Martill *et al.*, 2020).

51 In China, tapejarines are a common element of the famous Jehol Biota (e.g. Wang & Zhou,

52 2006). From the Yixian Formation (late Barremian – early Aptian), a single species, represented

53 by two specimens, has been described: *Eopteranodon lii* (Lü & Zhang, 2005; Andres & Ji, 2008;

54 Vullo *et al.*, 2012). It is, however, in the Jiufotang Formation (early Aptian) that a great

55 abundance of tapejarines is found. A total of 12 Jehol tapejarine specimens have been formally

56 reported in the literature (Wang & Zhou, 2003a; Li *et al.*, 2003; Lü & Zhang, 2005; Lü & Yuan,

57 2005, Lü *et al.*, 2006a,b,c, 2007, 2016; Liu *et al.*, 2015; Zhang *et al.*, 2019). Under the accounts

58 of Wu *et al.* (2017), at least further 9 undescribed specimens are currently deposited in

59 Paleontological Museum of Liaoning, and further 4 in Shandong University of Science and

60 Technology. According to our observations, further tens of specimens can be found in the

61 collections of other institutions such as the Beipiao Pterosaur Museum of China, the Dalian

62 Natural History Museum, and the Chaoyang National Geopark; bringing the total of recovered

63 specimens to over a hundred. Thus, tapejarines seem to represent an important element of the

64 Jehol Biota.

65 *Sinopterus dongi*, from the Jiufotang Formation (see Wang & Zhou, 2003a), was the first

66 tapejarid to be recovered from China, and is the type-species of the genus *Sinopterus*.

67 Subsequently, further six tapejarid species coming from the Jiufotang Fm. have also been

68 proposed: *Sinopterus gui*, *Sinopterus lingyuanensis*, *Huaxiapterus jii*, *Huaxiapterus corollatus*,

69 *Huaxiapterus benxiensis* and *Huaxiapterus atavismus* (see Wang & Zhou, 2003a; Li *et al.*, 2003;

70 Lü & Yuan, 2005; Lü *et al.*, 2006; 2007; 2016). The Jiufotang Fm. tapejarines are involved in a

71 complex series of taxonomic controversies, with the genus *Huaxiapterus* widely considered as a

72 junior synonym of *Sinopterus* (Wang & Zhou, 2006; Wang & Dong, 2008; Witton, 2013; Zhang

73 *et al.*, 2019; Naish *et al.*, 2021). At the species-level, basically two taxonomic schemes presently

74 exist for the genus *Sinopterus*, which could each be viewed as a conservative and an expansive

75 one. The conservative scheme, proposed by Witton (2013) and favored by Naish *et al.* (2021),

76 poses that Jiufotang tapejarines are oversplit, and that most, if not all, Jiufotang tapejarines are

77 members of an ontogenetic continuum of a single species, *Sinopterus dongi*. On the other hand,

78 the expansive scheme of Zhang *et al.* (2019) poses that Jiufotang tapejarines represent at least

79 five valid species within the genus *Sinopterus*: *S. dongi*, *S. corollatus*, *S. benxiensis*, *S.*

80 *lingyuanensis* and *S. atavismus*. The latter scheme derives from the scheme of Lü *et al.* (2016),

81 which posed that *Sinopterus* (with three species) and *"Huaxiapterus"* (with four species) are in

82 fact distinct at the generic level, what could thus be considered as a third scheme for the

83 taxonomy of the *Sinopterus* complex (a multi-generic, and also expansive, one).

84 Despite the abundance of tapejarid remains known from the Jiufotang Formation – and the

85   relevant taxonomic problems involved – not much has been published on the detailed,

86   comparative osteology of *Sinopterus*. Most of the reported specimens were only preliminarily

87   described and figured, to the exception of the recently published IVPP 22388-V, attributed to

88   *Sinopterus atavismus* (Zhang *et al.*, 2019). The detailed description of some of these specimens,

89   such as the holotype of *Sinopterus gui*, is further hampered by their poor preservation (Li *et al.*,

90   2003). This issue becomes particularly problematic due to the complicated taxonomic disputes

91   involved in the *Sinopterus* complex, which cannot be resolved before a detailed reassessment of

92   all known specimens.

93   Specimen D3072 is a newly reported specimen coming from the Jiufotang Formation,

94   represented by an almost complete, well-preserved postcranial skeleton. Due to its limb

95   proportions and pedal morphology, we attribute it to *Sinopterus dongi*, and defend such

96   attribution under both the conservative or the expansive taxonomic schemes for *Sinopterus*. The

97   main purpose of the present contribution is to offer a detailed account of the osteology of this

98   new specimen, improving knowledge on the anatomy of *Sinopterus dongi*. The importance of

99   such data lies in the need for detailed taxonomic revisions of this genus in the future, which will

100   require a better understanding of the osteology of *Sinopterus*.

101

102   **Material & Methods**

103   **Specimen and geological setting**

104   Specimen D3072 is permanently stored in the paleontological collection of the Dalian Natural

105   History Museum, in Dalian, Liaoning, China. The specimen was analyzed first-hand and under

106   lenses, measured with the use of calipers, and digitally photographed. Although it lacks precise

107   data on its origin or coordinates, it is catalogued as having been privately collected in the

108   Dapingfang locality (Dapingfang Town, Chaoyang City, Liaoning Province), in rocks belonging

109   to the Jiufotang Formation. The Jiufotang Formation (early Aptian), together with the underlying

110   Yixian Formation (late Barremian – early Aptian), belongs to the Jehol Group. Together (along

111   also with the Barremian Huajiying Formation of the Sichakou-Senjitu Basin), they yield the

112   Jehol Biota, famous for its paleontological richness and exquisite fossil preservation (e.g. Pan *et*

113   *al.*, 2013; Xu *et al.*, 2020). The Dapingfang locality has yielded several other Jiufotang Fm.

114   fossils of vertebrate taxa, such as: the azhdarchoid pterosaur *Chaoyangopterus zhangi* (Wang &

115   Zhou, 2003b), the istiodactyliform pterosaur *Hongshanopterus lacustris* (Wang *et al.*, 2008), the

116   istiodactylid *Nurhachius luei* (Zhou *et al.*, 2019), the dromaeosaurid *Microraptor gui* (Xu *et al.*

117   2003), the enanthiornithines *Dapingfangornis sentisorhinus* (Li *et al.*, 2006) and *Longipteryx*

118   *chaoyangensis* (Zhang *et al.*, 2001), the non-pygostylian avebrevicaudan *Sapeornis*

119   *chaoyangensis* (Zhou & Zhang, 2002a), the jeholornithiform *Jeholornis prima* (Zhou & Zhang,

120   2002b; 2003), the ornithuromorph *Yanornis martini* (Zhou *et al.*, 2004), and the squamate

121   *Yabeinosaurus tenuis* (Evans *et al.*, 2005).

122

123   **Anatomical terminology**

124   In the present study, anatomical terms follow Romerian nomenclature and orientation, using

125   anterior/posterior instead of cranial/caudal (e.g. Wilson, 2006). The standardization of the

126   orientation of wing elements is based on inferred flight position, following Bennett (2001).

127

128   **Reference phylogenetic proposal and systematic terminology**

129   The present study follows the reference phylogenetic proposal, and consequent systematic

130   terminology, that tapejarines and thalassodromines are sister-groups (Kellner & Campos, 2007;

131   Vullo *et al.*, 2012; Pêgas *et al.*, 2018; 2021). Together, they form the Tapejaridae *sensu* Kellner

132   & Campos (2007). Under alternative proposals, the Tapejaridae *sensu* Lü *et al.* (2006a) comprise

133   tapejarines *sensu* Kellner & Campos (2007) but excludes thalassodromines. Tapejarids *sensu* Lü

134   *et al.* (2006a) are interpreted as a basal group of azhdarchoids, with thalassodromines being more

135   closely related to azhdarchids + chaoyangopterids than to tapejarines – for such alternative

136   proposals, we refer the readers to Lü *et al.* (2008) and Andres *et al.* (2014).

137

138 **Institutional abbreviations**

139 **BMNH (=BPV),** Beijing Museum of Natural History, Beijing, China; **BXGM**, Benxi Geological

140 Museum, Benxi, China; **D**, Dalian Natural History Museum, Dalian, China; **GMN**, Geological

141 Museum of Nanjing, Nanjing, China; **IVPP**, Institute of Vertebrate Paleontology and

142 Paleoanthropology, CAS, Beijing, China; **JPM (=JZMP)**, Jinzhou Paleontological Museum,

143 Jinzhou, China; **PMOL (=LPM)**, Paleontological Museum of Liaoning, Shenyang, China;

144 **XHPM**, Xinghai Paleontological Museum, Dalian, China; **ZMNH**, Zhejiang Museum of Natural

145 History, Hangzhou, China.

146

Results

148 **Description of new specimen D3072**

149 **Generalities.** The specimen is represented by an almost complete postcranial skeleton preserved

150 on a single slab (Fig. 1, Table 1). The skull, pelvic region and femora are missing. These missing

151 elements (at least the pelvis, sacral vertebrae and femora) might, presumably, have been retained

152 in a counter-slab. Preservation quality varies throughout the skeleton. While some elements are

153 articulated and maintain their natural positions (such as the main wing bones, humerus, radius

154 and ulna, carpals, metacarpal IV and digit IV), some other elements are slightly displaced

155 (especially the scapula and coracoid, but also some small manual and pedal elements).

156 **Cervical series.** Apart from the atlas and axis, the remaining elements of the cervical series are

157 preserved. All mid-cervicals (cervicals III-VII) are exposed in left lateral view (Fig. 2). These

158 vertebrae are relatively elongate (length/height ratio 1.5–2.5; Table 1), slightly more so than in

159 *Tapejara wellnhoferi* or thalassodromines (length/height ratios of, respectively, ~2 and 0.9–1.9;

160 see Vila Nova *et al.*, 2015; Leal *et al.*, 2018), but less so than in chaoyangopterids (ratios 2–3;

161 see Wu *et al.*, 2017; Leal *et al.*, 2018) or azhdarchids (ratios 4–10; see Padian 1984; Andres *et al.*,

162 2014; Leal *et al.*, 2018; Naish & Witton, 2017; Pêgas *et al.*, 2021). Cervical IV is the longest one,

163 as measured from the tips of the prezygapophyses to the tips of the postzygapophyses (Table 1).

164   The preserved cervical vertebrae length formula is III < IV > V > VI > VII > VIII > IX. This

165   formula differs from other azhdarchoid taxa. In *Tapejara wellnhoferi*, cervicals IV and V are of

166   subequal length. According to Kellner & Hasegawa (1993), the same is true for *Tupuxuara*

167   *leonardii*, but for the sake of precision, we note that in fact cervical V is slightly longer than

168   cervical IV in this taxon (RVP, pers. obs.). The same is true for chaoyangopterids and

169   azhdarchids, in which cervical V is the longest (Lü *et al.*, 2008; Averianov, 2010; Wu *et al.* 2017;

170   Leal *et al.*, 2018). There are no mid-cervical ribs.

171   The neural spine is relatively low, similar to what is seen in *Tapejara* and thalassodromines (Vila

172   Nova *et al.*, 2015), which is lower than in pteranodontoids (e.g. Kellner & Tomida, 2000;

173   Bennett, 2001) but not as low as in chaoyangopterids (Wu *et al.* 2017; Leal *et al.*, 2018) nor as in

174   azhdarchids in which the neural spine is only a vestigial ridge (e.g. Averianov, 2010).

175   A single, small pneumatic foramen can be seen on the lateral surfaces of the third, fourth and

176   fifth cervical vertebrae; the status on the sixth and seventh is unclear due to crushing. This

177   foramen is located just below the zygapophyseal ridge, presumably near (ventral to) the contact

178   region between centrum and neural arch. This is similar to the condition seen in *Tapejara*

179   *wellnhoferi*, in which a single pneumatic foramen on the lateral surface of the mid-cervical

180   vertebrae is present (Vila Nova *et al*., 2015), while two or three are present in thalassodromines

181   (Vila Nova *et al*., 2015; Buchmann *et al.*, 2017) and none in chaoyangopterids and azhdarchids

182   (Averianov, 2010; Wu *et al.* 2017; Leal *et al.*, 2018; Buchmann & Rodrigues, 2019). Despite the

183   crushed nature of specimen D3072, the openings observed on the lateral surface of these

184   vertebrae match well in size, shape, and location the pneumatic foramina found in the mid-

185   cervical vertebrae of *Tapejara wellnhoferi* (Eck *et al.*, 2011; Vila Nova *et al.*, 2015), leading us

186   to interpret these openings in D3072 as pneumatic foramina as well. The tentative identification

187   of a possible lateral pneumatic foramina on the mid-cervicals of *Sinopterus* was already

188   mentioned by Vila Nova *et al.* (2015), inferred from a depression seen in cervical VII of the

189   holotype of *Sinopterus dongi*. Zhang *et al.* (2017) reported on the presence of this feature in

190   IVPP V 23387, a specimen they referred to *Sinopterus atavismus*. The same condition is seen in

191   the holotype of *Sinopterus lingyuanensis* (Lü *et al.*, 2016).

192   Some details of the mid-cervical vertebrae are obliterated due to crushing. The ventral margins

193   seem to be slightly damaged. In cervical VII, the ventral margin of the centrum is concave, with

194   a relatively large hypapophysis, similar to the condition seen in *Tapejara* (Vila Nova *et al.*,

195   2015). The status in other mid-cervicals is unclear. All mid-cervicals bear well-developed

196   postexapophyses. Cervicals VIII and IX are exposed in a somewhat ventrolateral view and not

197   much can be seen (Fig. 3).

198   **Dorsal series.** There are 11 preserved dorsal vertebrae (Fig. 3). The anterior margin is concave

199   and the posterior margin is convex. The first three dorsal vertebrae seem to exhibit fused centra

200   and neural arches. Dorsal vertebrae 4 and 5 are not very discernible due to crushing. Although

201   some overlying bones and sediment still obscure most of the centra, a contiguous series of

202   transverse processes can be seen, from dorsal vertebrae 1 through 13. A single centrum (probably

203   from dorsal vertebra 6, since is lies ventrally to the sixth dorsal neural arch) is displaced from

204   this contiguous series of neural arches, indicating it was not fused to its respective neural arch.

205   The posterior dorsal vertebrae (7–11) also exhibit an open suture between centra and neural

206   arches. This indicates that, while in mid-cervical vertebrae and anterior dorsal vertebrae the

207   centra were fused to the neural arches, the same was not true for mid- and posterior dorsals. A

208   similar condition was found in the juvenile *Tapejara wellnhoferi* specimen SMNK PAL 1137, in

209   which the preserved cervical vertebrae were entirely fused, while the single preserved dorsal

210   vertebrae lacked fusion between centrum and neural arch (Eck *et al.*, 2011). In dorsal vertebrae 1

211   and 2, it can be seen that a well-developed fossa is present at the ventral surface of the transverse

212   process base.

213   **Scapula.** The left scapula is preserved medial to the left humerus, in an approximately ventral

214   view (Fig. 3). It is not fused to the coracoid, which is displaced from it. Not much can be

215   observed due to crushing. The shaft of the scapula is wider than that of the coracoid. The scapula

216   is slightly bowed ventrodistally, similarly to *Tapejara wellnhoferi* (Eck *et al.*, 2011),

217   *Caupedactylus ybaka* (Kellner, 2013) or *Keresdrakon vilsoni* (Kellner *et al.*, 2019).

218   **Coracoid.** The left coracoid is exposed in dorsal view (Fig. 3). It is curved with an expanded

219   medial end. The medial end is bifid, terminating in an anterior and a posterior eminence, which

220   form the saddle-shaped sternal articulation. These two eminences are approximately equivalent

221   in size, unlike *Tapejara wellnhoferi* (Eck *et al.*, 2011), *Caupedactylus ybaka* (Kellner, 2013),

222   *Caiuajara dobruskii* (Manzig *et al.* 2014) or *Keresdrakon vilsoni* (Kellner *et al.*, 2019) in which

223   the posterior eminence is slightly larger than the anterior one.

224   **Humerus.** Both humeri are preserved approximately in ventral view (Fig. 4). The left humerus is

225   preserved in a better condition than the right one, in which the ulnar crest, deltopectoral crest and

226   distal region are slightly damaged. The shaft of the humerus is straight. The deltopectoral crest is

227   subrectangular in profile and is located proximally. The ventral margin is straight. It forms an

228   approximately perpendicular angle relative to the main shaft. This is similar to *Caupedactylus*

229   *ybaka* (Kellner, 2013) and *Tupuxuara leonardii* (Witton *et al.*, 2009), and slightly different from

230   *Tapejara wellnhoferi*, *Caiuajara dobruskii* and *Tupandactylus navigans*, in which the

231   deltopectoral crest is at a slightly oblique angle to the humeral shaft, ventromedially oriented

232   (Eck *et al.*, 2011; Manzig *et al.*, 2014; Beccari *et al.*, 2021). The region of the humeral head, in

233   ventral view, is marked by a triangular eminence. The ulnar crest is rounded and posterodorsally

234   flared (so that it is well visible in ventral view), similarly to *Tapejara wellnhoferi* and *Caiuajara*

235   *dobruskii* (Eck *et al.*, 2011; Manzig *et al.*, 2014). A distinct foramen is present on the ventral

236   proximal end of the humerus, close (slightly distal to) the humeral head, between the

237   deltopectoral and ulnar crests. This is similar to other azhdarchoids in general, as can be seen in

238   *Tapejara wellnhoferi* (Eck *et al.*, 2011), *Caiuajara dobruskii* (Manzig *et al.*, 2014),

239   *Tupandactylus navigans* (Beccari *et al.*, 2021), *Caupedactylus ybaka* (Kellner, 2013), *Tupuxuara*

240   *leonardii* (Kellner & Hasegawa, 1993), *Keresdrakon vilsoni* (Kellner *et al.*, 2019), and

241   azhdarchids (Lawson, 1975; Hone *et al.*, 2019). The humeral shaft slightly expands towards the

242   distal end. Two humeral epiphyses are present on the left side. They are unfused to the humerus

243   and preserved near the proximal region of the ulna. Since they are displaced from the humerus,

244   their relative orientation is unclear.

245   **Radius.** The ulna and radius are preserved parallel to each other on both sides. The diameter of

246   the ulna is larger than that of the radius. A precise ratio cannot be given, since the ulna partially

247   overlaps the radius on both sides, but the radius seems to be, roughly, not less than half the

248   diameter of the ulna. Not much can be observed on the right side, since the ulna and radius are

249   too compressed against each other, and the proximal and distal regions are slightly damaged. The

250   left side can be better observed, although crushing still obscures some details. The left radius and

251   ulna are exposed in an approximately anteroventral view.

252   The proximal region of the left radius bears a concave proximal margin (Fig. 5). The proximal

253   surface itself bears a cotyle. Two eminences can be seen, an anterodorsal and a posteroventral

254   one. The anterodorsal one (the biccipital process) is smaller than the posteroventral one and

255   projects only gently anterodorsally, similarly to *Tapejara wellnhoferi* (Eck *et al.*, 2011) and

256   *Jidapterus edentus* (Wu *et al.*, 2017). The posteroventral one, which is larger, projects

257   proximally, more so than in *Tapejara wellnhoferi* (Eck *et al.*, 2011) or *Jidapterus edentus* (Wu *et*

258   *al.*, 2017) in which it is less projected, or in *Pteranodon* in which it is rather inconspicuous

259   (Bennett, 2001). The distal end of the radius is slightly expanded, but not much can be seen due

260   to crushing.

261   **Ulna.** The left ulna is better preserved than the right one, as mentioned above. The shaft is

262   straight. On the proximal end, a dorsal, large eminence projects proximally, presumably for the

263   attachment of M. *triceps brachii* (Fig. 5). This eminence is particularly prominent, more so than

264   in *Tapejara wellnhoferi* (Eck *et al.*, 2011), *Jidapterus edentus* (Wu *et al.*, 2017) or *Pteranodon*

265   (Bennett, 2001). Ventral to this eminence, the capitular and trochlear cotyles can be seen,

266   separated by a discrete ridge. They both face proximally. Their shapes and dimensions cannot be

267   assessed confidently, since the region has been very compressed. On the distal end, two

1

268   collateral processes can be seen, a dorsal and a ventral one (Fig. 5). The dorsal one is much less

269   developed than the ventral one, similarly to *Tapejara wellnhoferi* (Eck *et al.*, 2011) and the

270   possible tapejarid *"Santanadactylus spixii"* (Wellnhofer, 1987; Kellner & Tomida, 2000) and

271   unlike *Pteranodon* in which they are roughly subequal (Bennett, 2001). The dorsal articular

272   surface, in the form of a gentle depression, can be seen on the distal surface of the dorsal

273   collateral process. The olecranon process is only slightly prominent, similar to *Pteranodon*

274   (Bennett, 2001) and unlike *"Santanadactylus spixii"* and *Tapejara wellnhoferi* in which it is

275   larger and more prominent (Wellnhofer, 1987; Eck *et al.*, 2011). Further details on the proximal

276   surface are unclear due to crushing.

277   **Carpals.** Both left and right carpal regions are preserved. On the left region, the bones are less

278   crushed, and it is clear that all carpal elements are unfused, although not much information can

279   be retrieved (Fig. 5). On the right side, the elements are very compressed against each other and

280   their limits thus became unclear, except for the preaxial carpal and pteroid which are slightly

281   displaced (Fig. 6). The pteroid can be seen on both sides. On the left side, it is almost complete,

282   lacking only the very apex tip. It is exposed in anterior view. It is thin, rod-like and elongated.

283   The shaft is gently bowed, and the base is slightly expanded. On the right side, only a small

284   fragment of the bone is preserved, also not in natural position.

285   **Metacarpals.** Metacarpals I-III are slender, thin, rod-like bones, while metacarpal IV is robust as

286   in other pterosaurs. Metacarpal I is not entirely preserved, as attested by a missing mid-shaft

287   portion (Fig. 6). Still, it extends for about 90% the distance between its distal tip and the carpal

288   region. The proximal tip seems to be damaged and it is likely that it extended further proximally,

289   possibly onto the carpal region, contacting it, as has been reported for the holotypes of

290   *Sinopterus dongi* and *"Huaxiapterus" jii* (Wang *et al.*, 2003; Lü & Yuan, 2005). Metacarpals II

291   and III are comparatively shorter, extending for about a third of metacarpal IV. They are pointed

292   proximally, and slightly expanded distally. Metacarpal IV is wider proximally than distally. The

293   distal region exhibits the typical trochlear-like morphology that is seen in pterosaurs, with a pair

294   of condyles, a dorsal one and a ventral one (e.g. Wellnhofer, 1978). Not much details can be seen

295   on the condyles due to crushing.

296   **Free digits.** On the right side, the manus is almost entirely preserved, except for the second

297   phalanx of digit 3 (Fig. 6). On the left side, only two phalanges are present for each digit, the two

298   phalanges of digit one and the two distal ones of digits 2 and 3 (Fig. 1). The digits become

299   progressively slightly longer from 1 to 3. The proximal phalanx of right digit 1 has a well-

300   developed trochlear-like articulation with two small condyles on the proximal tip. The condition

301   in the other proximal phalanges is unclear. The first digit bears only two phalanges (the proximal

302   phanalx and the ungual), as typical of pterosaurs (e.g. Wellnhofer, 1978). The second digit bears

303   three phalanges. On the third digit, only three phalanges are preserved, although the typical

304   condition in pterosaurs is the presence of four phalanges (e.g. Wellnhofer, 1978). The proximal

305   phalanx is disarticulated, displaced from its natural position. The two distalmost phalanges are

306   articulated to each other, from a distance from the proximal element. It is plausible that the third

307   phalanx of digit 3, which is typically small and square-like, has been displaced and possibly

308   obscured by the other elements. The manual claws are long and recurved. They are slightly

309   larger than the pedal claws, with relatively larger flexor tubercles as well.

310   **Wing digit.** Wing phalanges I-IV decrease in length progressively from I to IV (Fig. 1).

311   Phalanges 1-3 are straight. On the ventral surface of the proximal end of the right first phalanx,

312   two pneumatic openings are present, one on the posterior region and another on the anterior

313   region. Such feature has only ever been reported for the azhdarchoid *Keresdrakon vilsoni* (see

314   Kellner *et al.*, 2019). The fourth wing phalanx (as seen on both left and right sides) is

315   distinctively curved, as seen in *Eopteranodon lii* (Lü & Zhang, 2005; Lü *et al.*, 2006b) and the

316   holotypes of *Sinopterus dongi* (Wang & Zhou, 2003a), *S. jii* (Lü *et al.*, 2005) and *"H."*

317   *atavismus* (Lü *et al.*, 2016), but unlike *"Huaxiapterus" corollatus* in which it is straighter (Lü *et*

318   *al.*, 2006a).

319   **Tibia.** The right tibia is highly damaged, with displaced splints of crushed bone along its shaft.

320   The left tibia lacks the proximal region. As can be seen on both sides, neither the fibula nor the

321   proximal tarsals are fused to the tibia (Fig. 7). The tibia is broader proximally than distally.

322   **Fibula.** On both sides, it can be seen that the fibula is not fused to the tibia. The fibula is present

323   as a very thin, elongate bone, parallel to the tibia. It runs through, approximately, a third the

324   length of the tibia.

325   **Tarsus.** The tarsus can be observed on both sides (Fig. 7). Two proximal and two distal elements

326   are present on the left pes, all slightly displaced from their presumed natural positions. On the

327   right pes, the lateral proximal tarsal and both distal tarsals are preserved. The medial proximal

328   tarsal is not preserved. A small, rounded, unidentified bone is present. The proximal tarsals are

329   not fused to the tibia. On both sides, the lateral proximal tarsal is approximately rectangular and

330   is the largest tarsal element, as in IVPP V 23388-V (Zhang *et al.* 2019).

331   **Metatarsus.** Metatarsals I-IV are elongate, slender bones, slightly expanded at the ends (Fig. 7).

332   The proximal ends are broader than the distal ones, particularly in metatarsal IV. They are

333   progressively shorter from I to IV, as in the holotype of *Sinopterus dongi* (Wang & Zhou, 2003a)

334   and unlike other purported species of the *Sinopterus* complex (Zhang *et al.*, 2019). Metatarsal V

335   is reduced and hook-shaped, with a broad proximal region and a pointed distal apex. It articulates

336   with the lateral distal tarsal.

337   **Pedal digits.** The pedal formula can be inferred to be 2-3-4-5-1 (Fig. 7). The length ratio of

338   metatarsal III to tibia is 0.24. The pedal claws and the manual claws have roughly the same

339   shape, except that the manual claws are slightly larger and bear slightly larger flexor tubercles. A

340   keratinous ungual sheath is preserved on right pedal digit 4 (Fig. 7). The fifth digit is represented

341   by a single, extremely reduced phalanx, which is preserved on the left side.

342

343   **Discussion**

344 **Identification of specimen D3072**

345   Based on the relatively low level of postcranial bone fusion, it is clear that specimen D3072

346 is a juvenile. The new specimen lacks fusion of: the humeral epiphyses, scapulocoracoid, the

347 extensor tendon process of the first wing phalanx, the carpal elements, tibia and fibula, tibia and

348 proximal tarsals, and neural arches and centra of most dorsal vertebrae. The only postcranial

349 elements that are fused are the neural arches and centra of cervical vertebrae and anterior dorsal

350 vertebrae. Despite the uncertainties surrounding studies on the ontogeny of pterosaurs (see

351 Kellner, 2015; Dalla Vecchia, 2018) and reptiles overall (Griffin *et al.*, 2020), such low level of

352 skeletal fusion is indicative of a juvenile nature for this specimen (e.g. Bennett, 1993; Kellner,

353 2015; Dalla Vecchia, 2018; Griffin *et al.*, 2020). With a wingspan of about 1134 mm, D3072 is

354 similar in size to holotype of *Sinopterus dongi*, which is also a juvenile, with 1200 mm in

355 wingspan (Wang & Zhou, 2003a), and slightly larger than other juveniles such as the holotypes

356 of *S. gui* (with ~800 mm in wingspan; Li *et al.*, 2003) and *"H." atavismus* (~850 mm in

357 wingspan; Lü *et al.*, 2016). These are substantially larger than the possible near-hatchling

358 *Sinopterus* specimen represented by the holotype of *Nemicolopterus crypticus* (Witton, 2013;

359 Naish *et al.*, 2021), with a wingspan of ~250 mm. In contrast, D3072 is considerably smaller

360 than subadult specimens referred to the genus *Sinopterus* such as BXGM V0011 and IVPP V

361 23388, both with 1600 mm in wingspan (Lü *et al.*, 2007; Zhang *et al.*, 2019), or the adult

362 specimen D2525, with 2000 mm in wingspan (Lü *et al.*, 2006c).

363   The new specimen D3072 is flattened, preserved on a slab, as typical of Jehol fossils (e.g.

364 Pan *et al.*, 2013; Xu *et al.*, 2020) and many other pterosaur remains from around the world (e.g.

365 Beccari *et al.*, 2021). This frequent preservation style in pterosaurs turns anatomical comparisons

366 relatively hard, since it limits what bone surfaces can, or not, be viewed (e.g. in D3072, the

367 anterior and posterior views of the cervical vertebrae cannot be seen, nor the distal surface of the

368 humerus). Despite this obstacle, there are a number of observable features in specimen D3072

369 that allow its identification. It exhibits a subrectangular, non-warped deltopectoral crest of the

370 humerus, typical of the Tapejaroidea *sensu* Kellner (2003). Specimen D3072 further exhibits

371 features that are found in tapejarines such as mid-cervical vertebrae comparatively short with

372 low (but not ridge-like) neural spines and a single pneumatic foramen on the lateral surface (Vila

373 Nova *et al.*, 2015), as well as a dorsally flared ulnar crest of the humerus similar to *Tapejara* and

374 *Caiuajara* (Eck *et al.*, 2011; Manzig *et al.*, 2014). Together, all of these features are found only

375 in tapejarines such as *Tapejara* (e.g. Eck *et al.*, 2011; Vila Nova *et al.*, 2015), *Caiuajara*

376 (Manzig *et al.*, 2014) and *Sinopterus* (Wang & Zhou, 2003a; Lü *et al.*, 2016; Zhang *et al.*, 2019).

377 Limb proportions also match the typical condition seen in tapejarines, including *Sinopterus*

378 *dongi* (see Vila Nova *et al.*, 2012).

379   The fact that specimen D3072 is a tapejarine coming from the Jiufotang Formation indicates

380 that it likely belongs within the *Sinopterus* complex. The next question is whether it matches, or

381 not, any of the proposed species of *Sinopterus*. Under the expansive scheme defended by Zhang

382 *et al.* (2019), there is reason to regard D3072 as a specimen of *Sinopterus dongi*: this new

383 specimen exhibits a metatarsal I longer than metatarsals II-IV, which are progressively shorter.

384 This feature is absent in other proposed species of the genus, and is suggested as a diagnostic

385 feature of *Sinopterus dongi* under the expansive scheme (Zhang *et al.*, 2019). Furthermore,

386 regarding limb proportions, specimen D3702 closely matches the holotype of *Sinopterus dongi*,

387 (Wang & Zhou, 2003; Vila Nova & Sayão, 2012; see also Fig. 8). Under the conservative

388 scheme proposed by Witton (2013) and preliminarily defended by Naish *et al.* (2021), there is

389 also no reason to regard D3072 as distinct from the type-species *Sinopterus dongi*, with which it

390 shares pedal morphology and similar limb proportions. Thus, under either scheme, specimen

391 D3072 can confidently be attributed to the species *Sinopterus dongi*. How many further

392 *Sinopterus* species are valid or not, as well as their respective diagnostic features, are matters to

393 be explored elsewhere, pending detailed accounts of the comparative osteology of further

394 specimens.

395

Comments on the osteology of *Sinopterus dongi* and implications

The new specimen D3072 sheds fresh light on the osteology of *Sinopterus dongi*, corroborating previous suggestions and revealing new data. For instance, Vila Nova *et al.* (2015) were the first authors to suggest that pneumatic foramina were most likely present on the lateral surface of the centrum in *Sinopterus*, which were previously regarded as absent (Lü *et al.*, 2006b; Liu *et al.*, 2015). Later, Zhang *et al.* (2019) reported on the presence of this feature for IVPP V 23388 (therein referred to *S. atavismus*), but refrained from attesting its presence in other species of *Sinopterus*. In D3072, this feature is clearly preserved, suggesting that it was most likely common for all potential *Sinopterus* species. Specimens where it cannot be seen are probably simply affected by taphonomy, such as the holotype of *S. dongi*, as suggested by Vila Nova *et al.* (2015).

A purportedly distinctive scapula, described as strongly curved, has been considered as a diagnostic feature of *Sinopterus* (Wang & Zhou, 2003a; Zhang *et al.*, 2019), although it has not been demonstrated how such strong curvature differs from what is seen in other pterosaurs. If compared to other tapejarines, the curvature seen in the scapula of *Sinopterus dongi* (as seen from anterior or posterior views) is comparable to what is seen in *Tapejara wellnhoferi* (Eck *et al.*, 2011), *Caupedactylus ybaka* (Kellner, 2013) and *Caiuajara dobruskii* (Manzig *et al.*, 2014). If compared to other azhdarchoids, it is also comparable to the chaoyangopterid *Jidapterus edentus* (Wu *et al.*, 2017).

The coracoid, in turn, does seem to be distinctive in *Sinopterus dongi* if compared to other tapejarines. The coracoid of D3072 is notably bowed in dorsal view, more so than in *Tapejara*, *Caupedactylus* or *Caiuajara* (Eck *et al.*, 2011; Kellner, 2013; Manzig *et al.*, 2014). The proximal pair of eminences also exhibit a distinguishing condition, being similar in size, unlike *Tapejara*, *Caupedactylus* or *Caiuajara* in which posterior eminence is slightly larger than the anterior one. The condition in further proposed species of the *Sinopterus* complex remains to be described. This feature is thus of interest for future comparative studies involving Jiufotang tapejarines.

422   The overall anatomy of the humerus agrees well with *Tapejara* (see Eck *et al.*, 2011) and

423   *Caiuajara* (see Manzig *et al.*, 2014), due to the presence of an approximately straight shaft, a

424   rectangular deltopectoral crest, a humeral head eminence that is triangular in ventral view, and a

425   rounded, dorsally flared ulnar crest. This last character is absent in other azhdarchoids such as

426   *Caupedactylus* (Kellner, 2013), *Tupuxuara* (Witton *et al.*, 2009) and azhdarchids (Witton *et al.*,

427   2009) in which the ulnar crest is trapezoidal and posteriorly oriented, and this feature is thus of

428   potential phylogenetic relevance for tapejarines. Furthermore, *Sinopterus dongi* differs from

429   *Tapejara*, *Caiuajara* and *Tupandactylus* in exhibiting a deltopectoral crest of the humerus which

430   is perpendicular to the humeral shaft, while in *Tapejara*, *Caiuajara* and *Tupandactylus* it is

431   slightly oblique, slanting proximally (Eck *et al.*, 2011; Manzig *et al.*, 2014; Beccari *et al.*, 2021;

432   see also Fig. 9). Future comparative and phylogenetic studies should take these features into

433   account.

434   In the new specimen D3072, metacarpal I is very elongate and, as mentioned above,

435   probably contacted the carpus, as in the holotypes of *Sinopterus dongi* and *"Huaxiapterus" jii*

436   (Wang *et al.*, 2003; Lü & Yuan, 2005). This feature is worthy of further investigation, since a

437   short metacarpal I (extending for only a third of the length of metacarpal IV) is a potential

438   distinguishing feature between *"Huaxiapterus"* (as in the holotypes of *"H." benxiensis* and *"H."*

439   *corollatus*) and other *Sinopterus* species (Kellner & Campos, 2007). Future assessments of the

440   holotypes of *"H." benxiensis* and *"H." corollatus* are needed in order to verify this feature, by

441   investigating whether it is a natural feature or a potential preservation artifact.

442   Interestingly, the proximal region of the first wing phalanx of D3072 presents two ventral

443   pneumatic foramina, an anterior and a posterior one. This differs from other tapejarines such as

444   *Tapejara wellnhoferi* (Eck *et al.*, 2011), *Caupedactylus ybaka* (Kellner, 2013) and *Caiuajara*

445   *dobruskii* (Manzig *et al.*, 2014). It also differs from the thalassodromine *Tupuxuara leonardii*

446   (RVP, pers. obs.) and the chaoyangopterid *Jidapterus edentus* (Wu *et al.*, 2017), in which a

447   single foramen is present. A pair of foramina on the ventral side of the first wing phalanax

448   proximal region has been reported only for the azhdarchoid *Keresdrakon* (Kellner *et al.*, 2019).

449   Because of this peculiarity, it is worth investigating how widespread is this feature within

450   Jiufotang tapejarines, what may prove useful in future revisions of the *Sinopterus* complex.

451   Another interesting feature observable in the new specimen D3072 is the ungual sheath

452   preserved on the right pedal digit 4 (Fig. 7). The sheath extends for about 50 mm, which is about

453   85% the length of the bony ungual. Keratinous sheaths in tapejarid unguals were previously

454   known only from an incomplete skeleton from the Crato Formation, SMNK PAL 3830, which

455   also exhibits an elongate and well-recurved ungual sheath (Frey *et al.*, 2003). Specimen D3072

456   represents the first case of ungual sheath preservation in a Chinese tapejarid. Tapejarine

457   tapejarids such as *Sinopterus* specimens from the Jiufotang Formation, as well as SMNK PAL

458   3830, are known to exhibit ungual phalanges that are particularly robust and recurved if

459   compared to other pterosaurs such as pteranodontoids, azhdarchids and chaoyangopterids (Wu *et*

460   *al.*, 2017). The robust, recurved unguals of tapejarines have been interpreted as potentially

461   related to scansorial or arboreal habits, by favoring climbing of tree trunks (Wang & Zhou,

462   2003a). This interpretation was corroborated by morphometric analyses by Wu *et al.* (2017),

463   which revealed that, while chaoyangopterid unguals are consistent with those of ground-dwelling

464   tetrapods, those of tapejarines were consistent with those of tetrapods with specialized claws for

465   arboreal, scansorial, or predatory lifestyles (Wu *et al.*, 2017). The new specimen D3072 shows

466   that, in life, the pedal claws of *Sinopterus* were substantially longer and more recurved than

467   suggested by bone alone (as in SMNK PAL 3830), due to a significantly elongate horny sheath.

468   This further highlights the specialized morphology of tapejarine unguals, possibly related to

469   arboreal or scansorial habits (Wu *et al.*, 2017).

470

471   **Short comments on the *Sinopterus* complex**

472   Albeit relatively recent, the taxonomic history of the genus *Sinopterus* is convoluted. Since

473   the description of *Sinopterus dongi* (Wang & Zhou, 2003a), further 6 species were named until

474   2016 (see Lü *et al.*, 2016). Witton (2013) raised the concern that all Jiufotang tapejarines could

475   represent an ontogenetic continuum of a single species (including also *Nemicolopterus crypticus*,

476   interpreted as a potential hatchling specimen). Later on, further two new species were proposed:

477   *Sinopterus lingyuanensis* and *"Huaxiapterus" atavismus* (Lü *et al.*, 2016), which were later

478   regarded as valid (both under the genus *Sinopterus*) by Zhang *et al.* (2019), who recognized at

479   least five valid species for *Sinopterus*. More recently, Naish *et al.* (2021) corroborated the

480   proposition of Witton (2013) that most, if not all, proposed species could be conspecific

481   (including the most recently named ones, *Sinopterus lingyuanensis* and *"Huaxiapterus"*

482   *atavismus*). These authors demonstrated that all Jiufotang tapejarines seemed to fall within a

483   single spectrum of variation, as demonstrated by trends in limb and crest proportions (Naish *et*

484   *al.*, 2021). However, they expressed caution regarding this proposition. Naish *et al.* (2021)

485   noticed that the holotype of *"Huaxiapterus" corollatus* seems to be an outlier regarding limb

486   proportions and, thus, could represent a second taxon. These authors further reiterated that,

487   before the taxonomy of the *Sinopterus* complex can be resolved, a detailed anatomical

488   reassessment of the known specimens is needed (Naish *et al.*, 2021).

489   In the present work, we concur with the observations and preliminary conclusions provided

490   by Naish *et al.* (2021) regarding these issues. We regard that there is strong evidence for a

491   taxonomic oversplitting in the *Sinopterus* complex, although it is still possible that more than one

492   taxon is present in the known sample of Jiufotang tapejarines (see Naish *et al.*, 2021). In order to

493   try to untangle the *Sinopterus* complex, a detailed comparative reassessment of all known

494   specimens is thus paramount. However, before known specimens can be compared, detailed

495   accounts of their osteology need to be provided. So far, few works have focused on the detailed

496   osteological description of *Sinopterus* specimens (e.g. Zhang *et al.*, 2019). Detailed osteological

497   redescriptions are thus much needed for most of the known specimens (such as the types of

498   *Sinopterus gui*, *Sinopterus lingyuanensis* and *Huaxiapterus atavismus*). Given the importance of

499   osteological descriptions as foundations for subsequent taxonomic decisions and systematic

500   studies, in the present contribution we aimed at providing osteological data for the new specimen

501   D3072.

502   Here, we corroborate the presence of several features in *Sinopterus dongi*: pneumatic

503   foramina piercing the lateral surface of mid-cervical vertebrae, a metacarpal I reaching the

504   carpus, and a metatarsal I longer than subsequent metatarsals.   Based on the configuration of

505   metacarpal I, it does seem plausible that multiple species of *Sinopterus* could be present in the

506   Jiufotang assemblage, and not a single one. Further examination of the already known specimens,

507   with detailed descriptions, are needed in order to confirm whether the variation in metacarpal I is

508   natural or, perhaps, preservational. Based on metatarsal proportions, it does also seem plausible

509   that not all *Sinopterus* specimens are conspecific, and that, instead, more than one species is

510   present. Still, detailed accounts of these variations still need to be performed taking into account

511   the entire sample of known specimens.

512   From this point on, further anatomical accounts concerning the other proposed species must

513   be made. With time, this should allow a better understanding of osteological variation in the

514   *Sinopterus* complex and, subsequently, lead to a revised taxonomic scheme for the genus.

515   Hopefully this study will serve as a comparative basis for future works focusing on the osteology

516   and taxonomy of the *Sinopterus* complex.

517

Conclusions

519   The new specimen D3072 represents a postcranial skeleton of a Jiufotang tapejarine. Under both

520   the conservative and expansive taxonomic approaches that presently exist regarding the

521   *Sinopterus* complex, specimen D3072 is attributable to *Sinopterus dongi*, with which it shares

522   almost identical limb proportions and pedal morphology, with metatarsal I being the longest. The

523   osteological description we provide for this new specimen sheds new light on the anatomy of

524   *Sinopterus*, which should be helpful for future systematic studies as well as a taxonomic revision

525   of the *Sinopterus* complex.

526   In the present study, we confirm the presence of pneumatic foramina on the lateral surface of

527   mid-cervical vertebrae in *Sinopterus dongi*. We further report that this taxon distinguishes itself

528   from *Tapejara wellnhoferi* (the next best-known tapejarine so far) in that cervical IV is the

529   longest one, the two proximal coracoid eminences are similar in size, the deltopectoral crest of

530   the humerus is perpendicular to the humeral shaft, and that two ventral pneumatic foramina are

531   present on the proximal region of wing digit 1. We also note that *Sinopterus dongi* shares with

532   *Tapejara wellnhoferi*, as well as *Caiuajara dobruskii*, some features that are absent outside of the

533   Tapejarinae within azhdarchoids, such as a rounded and dorsally flared ulnar crest of the

534   humerus, a single and small pneumatic foramen on the mid-cervical vertebrae, and a well-

535   developed hypapophysis. We further report for the first time an ungual sheath in a pedal ungual

536   of *Sinopterus dongi*. It demonstrates that these structures were well-developed in this taxon,

537   further enhancing the elongation and the curvature of the pedal claw, similar to the indeterminate

538   Crato tapejarid SMNK PAL 3830.

539   The conditions of all of these features remain to be assessed in other purported species of the

540   *Sinopterus* complex, as well as on other tapejarids that were only preliminarily described such as

541   *Caiuajara dobruskii* (Manzig *et al.* 2014) and *Tupuxuara leonardii* (Kellner & Hasegawa, 1993),

542   and also taxa for which postcranial skeletons are still unknown (such as *Tupandactylus* spp. or

543   *Europejara olcadesorum*). Accounts on the osteology of these other forms will be needed in

544   order to assess potential diagnostic and phylogenetic signals in these features, which is possibly a

545   promising issue to explore. We hope the osteological data presented here will serve as basis for

546   comparative studies exploring further tapejarines overall, and especially those from the Jiufotang

547   Formation.

548

549   **Acknowledgements**

550 For access to specimens under their care, C.S. thanks Fangfang Teng (XHPM); R.V.P thanks

551 Xiaolin Wang (IVPP), Shunxing Jiang (IVPP), Dieter Schreiber (SMNK), and Eberhard Frey

552 (SMNK); and X.Z. thanks Xinsheng Jin (ZMNH), Qiannan Zhang (BMNH), Shaowen Zhang

553 (CAGS), Jun Zhang (BXGM), Honggang Huo (BXGM), and Deyu Sun (JPM). R.V.P thanks

554 Maria E. Leal, Lucy Souza and Kamila Bandeira for fruitful discussions.

555

556 **References**

557

558 **Andres B, Ji Q. 2008.** A new pterosaur from the Liaoning Province of China, the phylogeny of

559   the Pterodactyloidea, and the convergence in their cervical vertebrae. Palaeontology, 51:

560   453–469.

561 **Andres B, Clark JM, Xu X. 2014.** The earliest pterodactyloid and the origin of the

562   group. Current Biology, 24(9): 1011-1016.

563 **Averianov AO. 2010.** The osteology of *Azhdarcho lancicollis* Nessov, 1984 (Pterosauria,

564   Azhdarchidae) from the late Cretaceous of Uzbekistan. Proceedings of the Zoological

565   Institute RAS, 314(3): 264-317.

566 **Bennett SC. 1993.** The ontogeny of *Pteranodon* and other pterosaurs. Paleobiology, 19(1): 92-

567   106.

568 **Bennett SC. 2001.** The osteology and functional morphology of the Late Cretaceous pterosaur

569   *Pteranodon* Part I. General description of osteology. Palaeontographica Abteilung A

570   2001:1–112.

571 **Buchmann R, Rodrigues T, Polegario S, Kellner AWA. 2018.** New information on the

572   postcranial skeleton of the Thalassodrominae (Pterosauria, Pterodactyloidea,

573   Tapejaridae). Historical Biology, 30(8): 1139-1149.**Buchmann R, Rodrigues T. 2019.**

574   The evolution of pneumatic foramina in pterosaur vertebrae. Anais Da Academia

575   Brasileira De Ciencias, 91.

576   **Dalla Vecchia FM. 2019.** *Seazzadactylus venieri* gen. et sp. nov., a new pterosaur (Diapsida:

577   Pterosauria) from the Upper Triassic (Norian) of northeastern Italy. PeerJ, 7: e7363.

578   **Evans SE, Wang Y, Li C. 2005.** The Early Cretaceous lizard *Yabeinosaurus* from China:

579   resolving an enigma. Journal of Systematic Palaeontology, 3: 319–335.

580   **Eck K, Elgin RA, Frey E. 2011.** On the osteology of *Tapejara wellnhoferi* Kellner 1989 and the

581   first occurrence of a multiple specimen assemblage from the Santana Formation, Araripe

582   Basin, NE-Brazil. Swiss Journal of Palaeontology, 130(2): 277.

583   **Frey E, Tischlinger H, Buchy MC, Martill DM. 2003.** New spec mens of Pterosauria (Reptilia)

584   with soft parts with implications for pterosaurian anatomy and locomotion. In: E.

585   Buffetaut and J.-M. Mazin (eds.), Evolution and Palaeobiology of Pterosaurs. Geological

586   Society of London, Special Publications, 217: 233–266.

587   **Griffin CT, Stocker MR, Colleary C, Stefanic CM, Lessner EJ, Riegler M, …, Nesbitt SJ.**

588   **2021.**   Assessing   ontogenetic   maturity   in   extinct   saurian   reptiles. Biological

589   Reviews, 96(2): 470-525.

590   **Hone DW, Habib MB, Therrien F. 2019.** *Cryodrakon boreas*, gen. et sp. nov., a Late

591   Cretaceous Canadian azhdarchid pterosaur. Journal of Vertebrate Paleontology, 39(3):

592   e1649681.

593   **Kellner AWA. 2003.** Pterosaur phylogeny and comments on the evolutionary history of the

594   group. Geological Society, London, Special Publications, 217(1): 105–137.

595   **Kellner AWA. 2013.** A new unusual tapejarid (Pterosauria, Pterodactyloidea) from the Early

596   Cretaceous Romualdo Formation, Araripe Basin, Brazil. Earth and Environmental

597   Science Transactions of the Royal Society of Edinburgh, 103(3-4): 409-421.

598   **Kellner AWA. 2015.** Comments on Triassic pterosaurs with discussion about ontogeny and

599   description of new taxa. Anais da Academia Brasileira de Ciências, 87: 669-689.

600   **Kellner AWA, Campos DA. 2007.** Short note on the ingroup relationships of the Tapejaridae

601   (Pterosauria, Pterodactyloidea). Boletim do Museu Nacional, Nova Série, Rio de Janeiro-

602   Brasil. Geologia, 75: 1–14.

Kellner AWA, Hasagawa Y. 1993. Postcranial skeleton of *Tupuxuara* (Pterosauria, Pterodactyloidea, Tapejaridae) from the Lower Cretaceous of Brazil. Journal of Vertebrate Paleontology, 13: 44A.

Kellner AWA, Tomida Y. 2000. Description of a new species of Anhangueridae (Pterodactyloidea) with comments on the pterosaur fauna from the Santana Formation (Aptian-Albian), Northeastern Brazil. National Science Museum, Tokyo, Monographs, 17: 1–135.

Kellner AWA, Weinschütz LC, Holgado B, Bantim RA, Sayao JM. 2019. A new toothless pterosaur (Pterodactyloidea) from Southern Brazil with insights into the paleoecology of a Cretaceous desert. Anais da Academia Brasileira de Ciências, 91.

Lawson DA. 1975. Pterosaur from the Latest Cretaceous of West Texas: Discovery of the largest flying creature. Science, 185: 947–948.

Leal MEC, Pêgas RV, Bonde N, Kellner AWA. 2018. Cervical vertebrae of an enigmatic pterosaur from the Crato Formation (Lower Cretaceous, Araripe Basin, NE Brazil). Geological Society, London, Special Publications, 455(1): 195-208.

Li JJ, Lü JC, Zhang BK. 2003. A new lower Cretaceous sinopterid pterosaur from Western Liaoning, China. Acta Palaeontologica Sinica, 42: 442–447.

Li L, Ye D, Dongyu H, Li W, Shaoli C, Lianhai H. 2006. New eoenantiornithid bird from the early cretaceous Jiufotang formation of Western Liaoning, China. *Acta Geologica Sinica-English Edition*, *80*(1), 38-41.

Liu DX, Zhou CF, Wang JQ, Li WG, Wei QW. 2015. New data on the cervical morphology of the Chinese tapejarine. Historical Biology, 27(6): 638-645.

Lü JC, Gao CL, Liu JY, Meng QJ, Ji Q. 2006b. New material of the pterosaur *Eopteranodon* from the Early Cretaceous Yixian Formation, western Liaoning, China. Geological Bulletin of China, 25: 555–571.

Lü JC, Gao YB, Xing LD, Li ZX, Sun ZY. 2007. A new species of *Huaxiapterus* from the Early Cretaceous of western Liaoning,China. Acta Geologica Sinica, 81(5): 683–687.

630 **Lü JC, Jin XS, Unwin DM, Zhao LJ, Azuma Y, Ji Q. 2006a.** A new species of *Huaxiapterus*
631   (Pterosauria: Pterodactyloidea) from the Lower Cretaceous of western Liaoning, China
632   with comments on the systematics of tapejarid pterosaurs. Acta Geologica Sinica, 80(3):
633   315–326.

634 **Lü JC, Liu JY, Wang XR, Gao CL, Meng QJ, Ji Q. 2006c.** New material of the pterosaur
635   *Sinopterus* (Reptilia: Pterosauria) from the Early Cretaceous Jiufotang Formation,
636   Western Liaoning, China. Acta Geologica Sinica, 80: 783–789.

637 **Lü JC, Teng FF, Sun DY, Shen CZ, Li GQ, Gao X, Liu HF. 2016.** The toothless pterosaurs
638   from China. Acta Geologica Sinica, 90(9): 2513–2525.

639 **Lü J, Unwin DM, Xu L, Zhang X. 2008.** A new azhdarchoid pterosaur from the Lower
640   Cretaceous of China and its implications for pterosaur phylogeny and
641   evolution. Naturwissenschaften, 95(9): 891–897.

642 **Lü JC, Yuan CX. 2005.** New tapejarid pterosaur from western Liaoning, china. Acta Geologica
643   Sinica, 79(4): 453-458.

644 **Lü JC, Zhang BK. 2005.** New pterodactyloid pterosaur from the Yixian Formation of western
645   Liaoning. Geological Review, 51: 458–462.

646 **Manzig PC, Kellner AWA, Weinschütz LC, Fragoso CE, Vega CS, Guimarães GB, Godoy**
647   **LC, Liccardo A, Ricetti JHZ, de Moura CC. 2014.** Discovery of a rare pterosaur bone
648   bed in a Cretaceous desert with insights on ontogeny and behavior of flying reptiles. PloS
649   one, 9(8): e100005.

650 **Martill DM, Green M, Smith RE, Jacobs ML, Winch J. 2020.** First tapejarid pterosaur from
651   the Wessex Formation (Wealden Group: Lower Cretaceous, Barremian) of the United
652   Kingdom. Cretaceous Research, 113: 104487.

653 **Naish D, Witton MP. 2017.** Neck biomechanics indicate that giant Transylvanian azhdarchid
654   pterosaurs were short-necked arch predators. PeerJ, 5: e2908.

655 **Naish D, Witton MP, Martin-Silverstone E. 2021.** Powered flight in hatchling pterosaurs:
656   evidence from wing form and bone strength. Scientific Reports, 11(1): 1-15.

657   **Nessov LA. 1984.** Pterosaurs and birds of the Late Cretaceous of Central Asia. Paläontologische
658   Zeitschrift, 1: 47–57.

659   **Pan YH, Sha JG, Zhou ZH, Fürsich FT. 2013.** The Jehol Biota: definition and distribution of
660   exceptionally preserved relicts of a continental Early Cretaceous ecosystem. Cretaceous
661   Research, 44: 30-38.

662   **Pêgas RV, Leal MEC, Kellner AWA. 2016.** A basal tapejarine (Pterosauria; Pterodactyloidea;
663   Tapejaridae) from the crato formation, Early Cretaceous of Brazil. PLoS One, 11(9):
664   e0162692.

665   **Pêgas RV, Holgado B, David LDO, Baiano MA, Costa FR. 2021.** On the pterosaur *Aerotitan*
666   *sudamericanus* (Neuquén Basin, Upper Cretaceous of Argentina), with comments on
667   azhdarchoid phylogeny and jaw anatomy. Cretaceous Research: 104998.

668   **Vila Nova BC, Sayão JM. 2012.** On wing disparity and morphological variation of the Santana
669   Group pterosaurs. Historical Biology, 24(5): 567-574.

670   **Vila Nova BC, Sayão JM, Langer MC, Kellner AWA. 2015.** Comments on the cervical
671   vertebrae of the Tapejaridae (Pterosauria, Pterodactyloidea) with description of new
672   specimens. Historical Biology, 27(6): 771-781.

673   **Vullo R, Marugán-Lobónm J, Kellner AWA, Buscalioni A, Fuente M, Moratalla JJ. 2012.**
674   A new crested pterosaur from the Early Cretaceous of Spain: The first European tapejarid
675   (Pterodactyloidea: Azhdarchoidea). PLoS ONE, 7: e38900.

676   **Wang L, Li L, Duan Y, Cheng SL. 2006.** A new istiodactylid pterosaur from western Liaoning.
677   Geological Bulletin of China, 25: 737–740.

678   **Wang XL, Campos DA, Zhou ZH, Kellner AWA. 2008.** A primitive istiodactylid pterosaur
679   (Pterodactyloidea) from the Jiufotang Formation (Early Cretaceous), northeast China.
680   Zootaxa, 1813: 1–18.

681   **Wang XL, Dong ZM. 2008.** Order Pterosauria. In: Li JL, Wu XC and Zhang FC (Eds), the
682   Chinese fossil reptiles and their kin, 2nd ed., Beijing: Sci Press, p: 215-234.

683   **Wang XL, Zhou ZH. 2003a.** A new pterosaur (Pterodactyloidea, Tapejaridae) from the Early

Cretaceous Jiufotang Formation of Western Liaoning, China and its implications for biostratigraphy. Chinese Science Bulletin, 48(1): 16-23.

Wang XL, Zhou ZH. 2003b. Two new pterodactyloid pterosaurs from the Early Cretaceous Jiufotang Formation of Western Liaoning, China. Vertebrata Palasiatica, 41: 34–41.

Wang XL, Zhou ZH. 2006. Pterosaur assemblages of the Jehol Biota and their implication for the Early Cretaceous pterosaur radiation. Geological Journal, 41(3-4): 405-418.

Wang XL, Campos DDA, Zhou ZH, Kellner AWA. 2008. A primitive istiodactylid pterosaur (Pterodactyloidea) from the Jiufotang Formation (Early Cretaceous), northeast China.

Wellnhofer P. 1978. *Handbuch der Paläoherpetologie. Teil 19: Pterosauria.* Stuttgart, Gustav Fischer Verlag.

Wellnhofer P. 1987. New crested pterosaurs from the Lower Cretaceous of Brazil. Mitteilungen der Bayerischen Staatssammlung für Paläontologie und historische Geologie, 27: 175-186.

Wilson JA. 2006. Anatomical nomenclature of fossil vertebrates: standardized terms or 'lingua franca'? Journal of Vertebrate Paleontology, 26(3): 511-518.

Witton MP. 2013. *Pterosaurs*. Princeton University Press.

Witton MP, Martill DM, Green M. 2009. On pterodactyloid diversity in the British Wealden (Lower Cretaceous) and a reappraisal of *"Palaeornis" cliftii* Mantell, 1844. Cretaceous Research, 30: 676–686.

Wu WH, Zhou CF, Andres B. 2017. The toothless pterosaur *Jidapterus edentus* (Pterodactyloidea: Azhdarchoidea) from the Early Cretaceous Jehol Biota and its paleoecological implications. PLoS One, 12(9): e0185486.

Xu X, Zhou ZH, Wang XL, Kuang XW, Zhang FC, Du XK. 2003. Four-winged dinosaurs from China. Nature, 421(6921): 335-340.

Xu X, Zhou ZH, Wang Y, Wang M. 2020. Study on the Jehol Biota: recent advances and future prospects. Science China Earth Sciences, 63(6): 757-773.

Zhang FC, Zhou ZH, Hou LH, Gu G. 2001. Early diversification of birds: evidence from a

711   new opposite bird. Chinese Science Bulletin, 46(11): 945–949

712 **Zhang XJ, Jiang SX, Cheng X, Wang XL. 2019.** New material of *Sinopterus* (Pterosauria,

713   Tapejaridae) from the Early Cretaceous Jehol Biota of China. Anais da Academia Brasileira

714   de Ciências, 91.

715 **Zhou CF. 2010.** New material of *Chaoyangopterus* (Pterosauria: Pterodactyloidea) from the

716   Early Cretaceous Jiufotang Formation of western Liaoning, China. Neues Jahrbuch fur

717   Geologie und Palaontologie-Abhandlungen, 257(3): 341.

718 **Zhou XY, Pêgas RV, Leal MEC, Bonde N. 2019.** *Nurhachius luei*, a new istiodactylid

719   pterosaur (Pterosauria, Pterodactyloidea) from the Early Cretaceous Jiufotang Formation of

720   Chaoyang City, Liaoning Province (China) and comments on the Istiodactylidae. PeerJ, 7:

721   e7688.

722 **Zhou ZH, Clarke J, Zhang FC, Wings O. 2004.** Gastroliths in *Yanornis*: an indication of the

723   earliest radical diet-switching and gizzard plasticity in the lineage leading to living

724   birds? Naturwissenschaften, 91(12): 571-574.

725 **Zhou ZH, Zhang FC. 2002a.** Largest bird from the Early Cretaceous and its implications for the

726   earliest avian ecological diversification. Naturwissenschaften, 89: 34–38.

727 **Zhou ZH, Zhang FC. 2002b.** A long-tailed, seed-eating bird from the Early Cretaceous of

728   China. Nature, 418: 405–409.

729 **Zhou ZH, Zhang FC. 2003.** *Jeholornis* compared to *Archaeopteryx*, with a new understanding

730   of the earliest avian evolution. Naturwissenschaften, 90: 220–225.

731

732 Figures

733 **Figure 1. Specimen D3072, general view.** (A) Photograph and (B) schematic drawing.

734 Abbreviations: cv, cervical vertebrae; co, coracoid; dv, dorsal vertebrae; dr, dorsal rib; fi, fibula;

735 h, humerus; mc, metacarpal; mt, metatarsal; pt, pteroid; ra, radius; sc, scapula; ti, tibia; ul, ulna;

736 wph, wing phanlanx.

737

738 **Figure 2. Specimen D3072, mid-cervical vertebrae.** (A) Photograph and (B) schematic

739   drawing. Abbreviations: c, cervical; hyp, hypapophysis; pf, pneumatic foramen; poex,

740   postexapophysis; poz, postzygapophysis; prz, prezygapophysis. Scale bar equals 10 mm.

741

742   **Figure 3. Specimen D3072, trunk region.** (A) Photograph and (B) schematic drawing.

743   Abbreviations: c, cervical; co, coracoid; d, dorsal; h, humerus; r, rib; sc, scapula.

744

745   **Figure 4. Specimen D3072, humerus.** Photograph of (A) left and (B) right humeri. Schematic

746   drawing of (A) left and (B) right humeri. Abbreviations: dpc, deltopectoral crest; h, head; pf,

747   pneumatic foramen; uc, ulnar crest. Scale bar equals 10 mm.

748

749   **Figure 5. Specimen D3072, radius and ulna.** Proximal region, (A) photograph and (B)

750   schematic drawing. Scale bar equals 10 mm. Distal region, (C) photograph and (D) schematic

751   drawing. Abbreviations: ca, carpal; capc, capitular cotyle; ctb, crest for M. *triceps brachii*; dclp,

752   dorsal collateral process; epi, epiphysis; h, humerus; ol, olecranon; pt, pteroid; ra, radius; troc,

753   trochlear cotyle; ul, ulna; vclp, ventral colateral process.

754

755   **Figure 6. Specimen D3072, right carpus and manus.** (A) Photograph and (B) schematic

756   drawing. Abbreviations: d, digit; dc, distal carpals; etp, extensor tendon process; lpc, lateral

757   proximal carpal; mc, metacarpal; mpc, medial proximal carpal; pt, pteroid; ra, radius; ul, ulna; pc,

758   preaxial carpal; pf, pneumatic foramen; ph, phanlanx; pt, pteroid. Scale bar equals 10 mm.

759

760   **Figure 7. Specimen D3072, pedes.** Right pes, (A) photograph and (B) schematic drawing. Left

761   pes, (C) photograph and (D) schematic drawing. Abbreviations: f, fibula; ldt, lateral distal tarsal;

762   lpt, lateral proximal tarsal; mdt, medial distal tarsal; mt, metatarsal; t, tibia; us, ungual sheath.

763   Scale bar equals 10 mm.

764

765

766   **Figure 8. Wing elements proportions (in percentage of total wing length) in selected**

767   **azhdarchoids.** Data source: *Sinopterus dongi* (holotype, IVPP V 13363; Wang & Zhou (2003a);

768   *Sinopterus "jii"* (holotype, GMN-03-11-001; Lü & Yuan, 2005); *S. atavismus* (holotype, XHPM

769   1009; Lü *et al.*, 2016); *Eopteranodon lii* (D2526, Lü *et al.*, 2006b); D2525 (Lü *et al.*, 2006c);

770 *"Huaxiapterus" benxiensis* (holotype, BXGM V0011; Lü *et al.*, 2007); *"Huaxiapterus"*
771 *corollatus* (holotype, ZMNH M8131), Lü *et al.* (2006a); *Tupandactylus navigans* (GP/2E 9266),
772 Beccari *et al.* (2021); *Caiuajara dobruskii* (composite), Manzig *et al.* (2014); *Jidapterus edentus*
773 (holotype, RCPS-030366CY), Wu *et al.* (2017); *Chaoyangopterus zhangi* (holotype, IVPP V
774 13397), Wang & Zhou (2003b); *Shenzhoupterus chaoyangensis* (holotype, HGM 41HIII-305A),
775 Lü *et al.* (2008). Abbreviations: d, digit; hol., holotype; McIV, metacarpal IV; ph, phalanx.
776
777

778 **Figure 9. Humerus morphology in tapejarines.** (A) *Caupedactylus ybaka*, right humerus in
779 anterior view, drawn from Kellner (2013). (B) D3072, left humerus in an approximately ventral
780 view. (C) *Tupandactylus navigans*, mirrored right humerus in posterior view, drawn from
781 Beccari *et al.* (2021). (D) *Caiuajara dobruskii*, mirrored left humerus in anterior view, drawn
782 from Manzig *et al.* (2014). (E) *Tapejara wellnhoferi*, right humerus in anterior view, drawn from
783 Eck *et al.* (2011). Notice the variation in the orientation of the deltopectoral crest, perpendicular
784 to humeral shaft in (A) and (B), and oblique in (C), (D) and (E). Scale bars equal 10 mm.
785

786 **Tables**

787 **Table 1. Measurements of the new specimen D3072.** Measurements given in milimeters.

788

789

790

Figure 1

Figure 1. Specimen D3072, general view.

(A) Photograph and (B) schematic drawing. Abbreviations: cv, cervical vertebrae; co, coracoid; dv, dorsal vertebrae; dr, dorsal rib; fi, fíbula; h, humerus; mc, metacarpal; mt, metatarsal; pt, pteroid; ra, radius; sc, scapula; ti, tibia; ul, ulna; wph, wing phanlanx.

Figure 2

Figure 2. Specimen D3072, mid-cervical vertebrae.

(A) Photograph and (B) schematic drawing. Abbreviations: c, cervical; hyp, hypapophysis; pf, pneumatic foramen; poex, postexapophysis; poz, postzygapophysis; prz, prezygapophysis. Scale bar equals 10 mm.
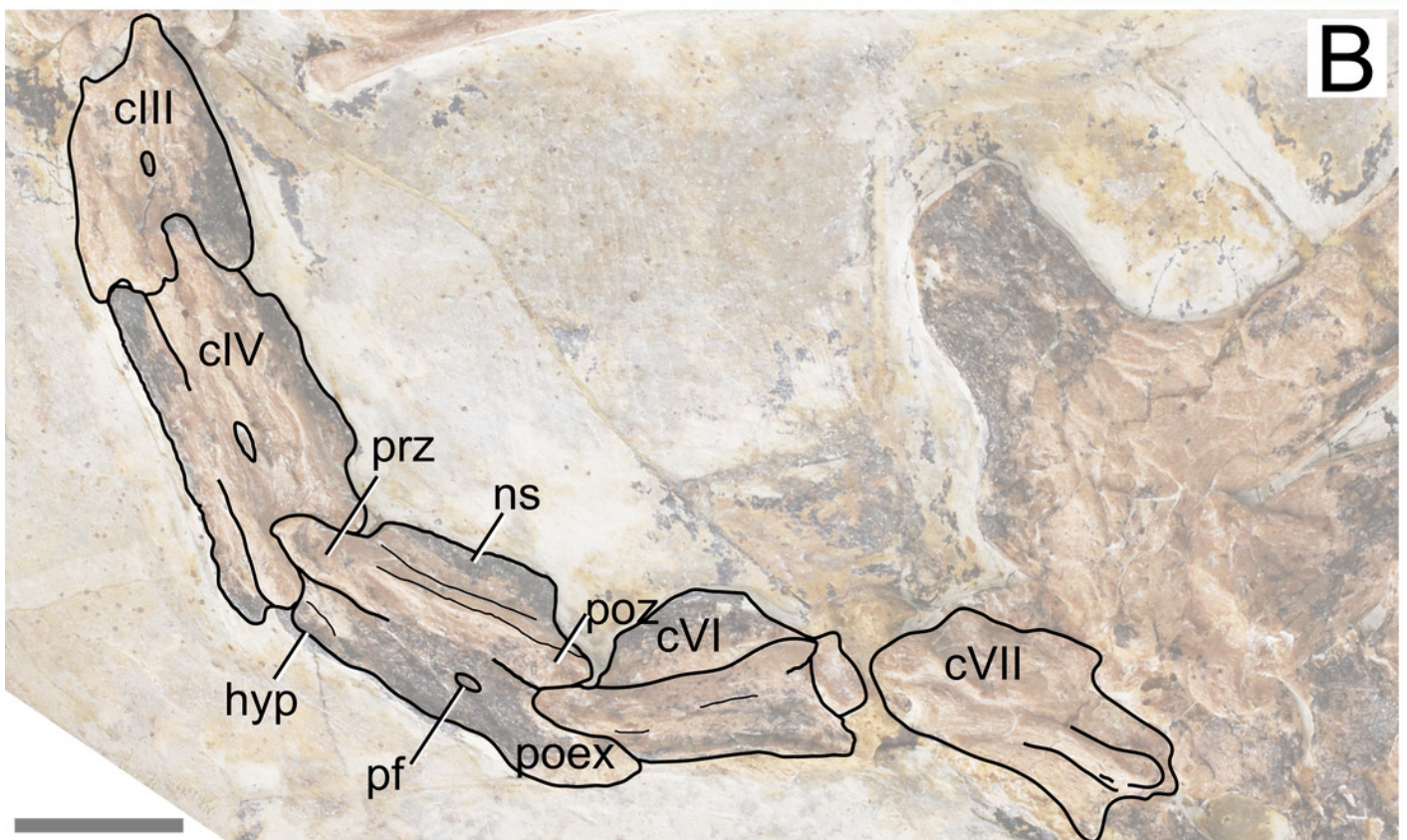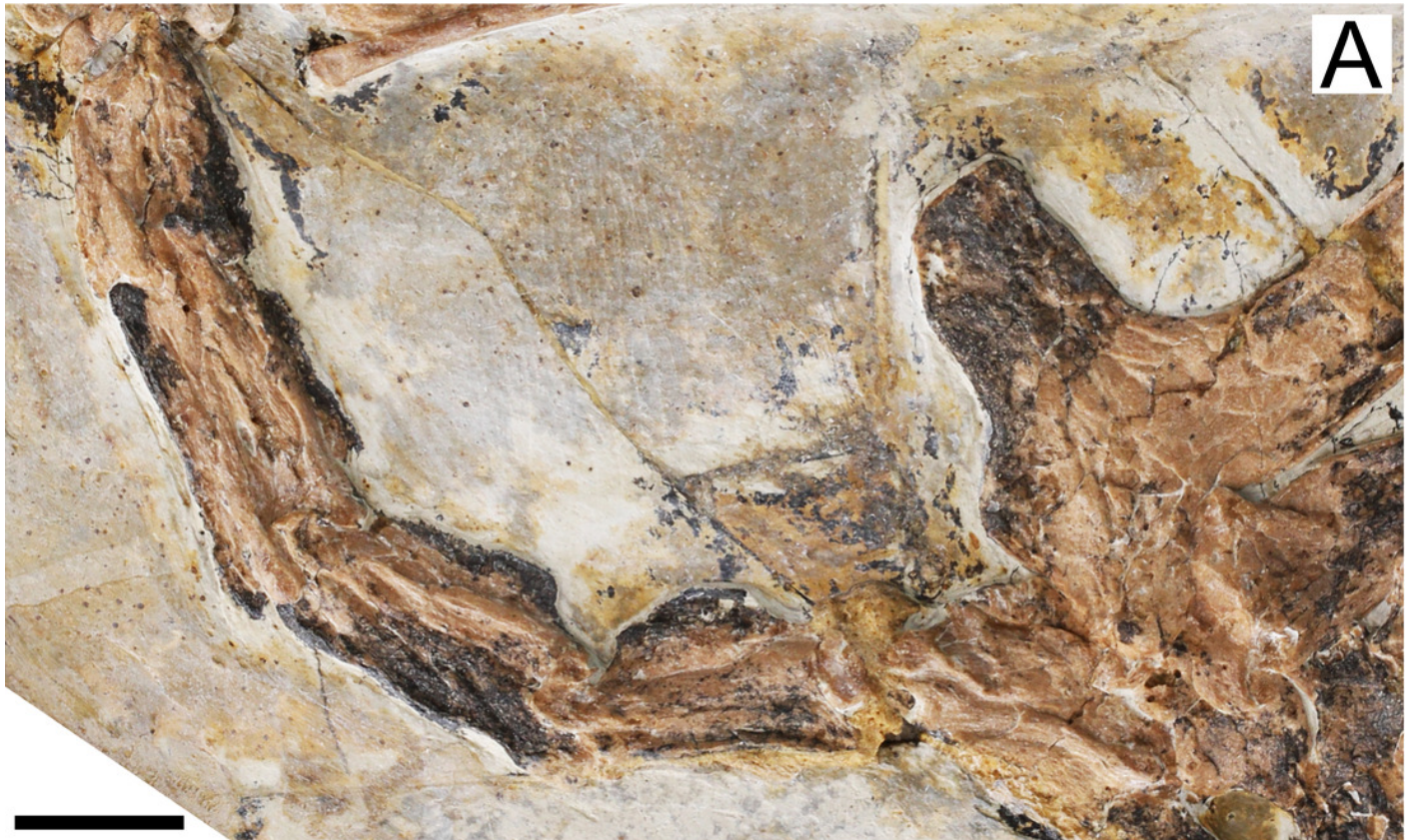
Figure 3

Figure 3. Specimen D3072, trunk region.

(A) Photograph and (B) schematic drawing. Abbreviations: c, cervical; co, coracoid; d, dorsal; h, humerus; r, rib; sc, scapula.
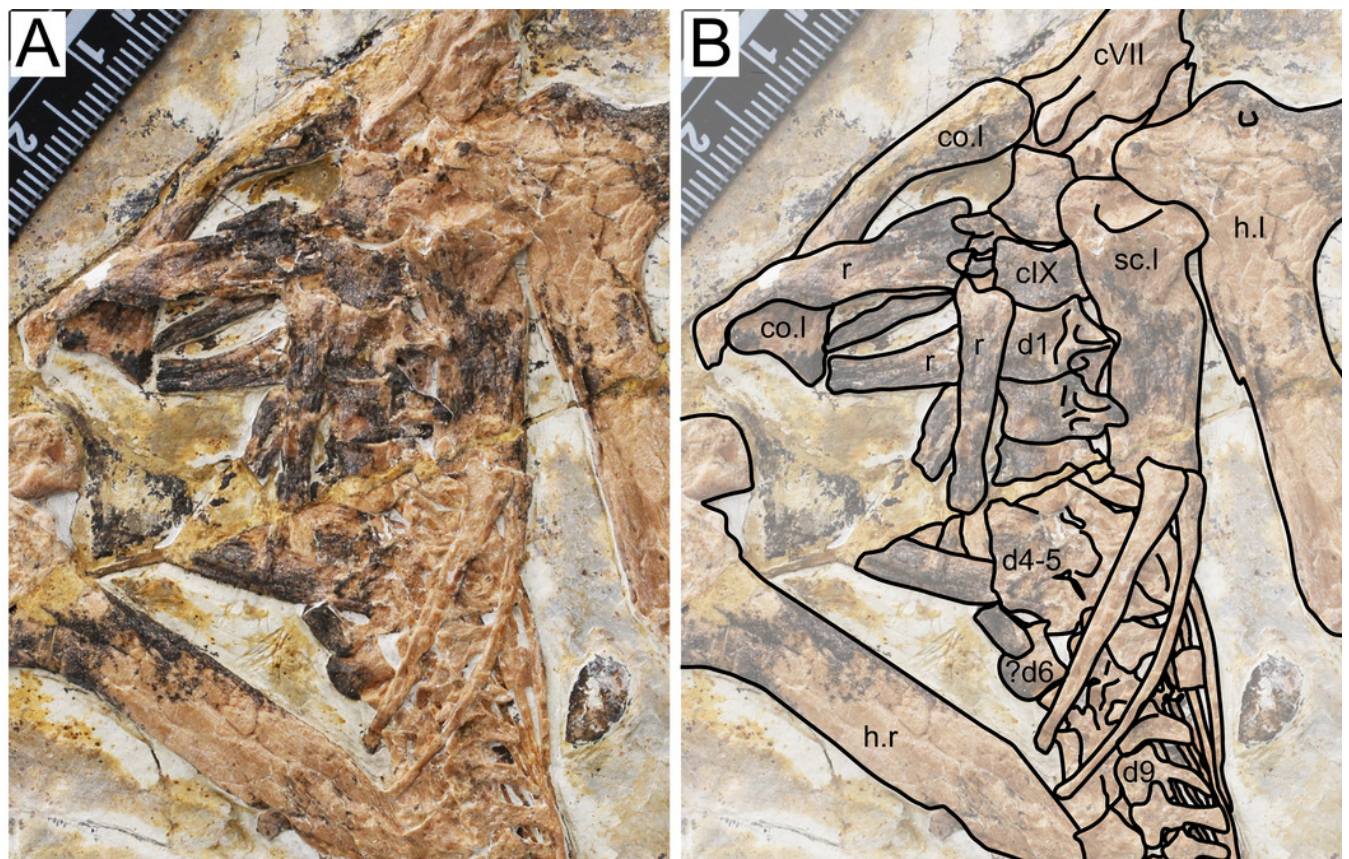
Figure 4

Figure 4. Specimen D3072, humerus.

Photograph of (A) left and (B) right humeri. Schematic drawing of (A) left and (B) right humeri. Abbreviations: dpc, deltopectoral crest; h, head; pf, pneumatic foramen; uc, ulnar crest. Scale bar equals 10 mm.

Figure 5

Figure 5. Specimen D3072, radius and ulna.

Proximal region, (A) photograph and (B) schematic drawing. Scale bar equals 10 mm. Distal region, (A) photograph and (B) schematic drawing. Abbreviations: ca, carpal; capc, capitular cotyle; ctb, crest for M. *triceps brachii*; dclp, dorsal collateral process; epi, epiphysis; h, humerus; ol, olecranon; pt, pteroid; ra, radius; troc, trochlear cotyle; ul, ulna; vclp, ventral colateral process.
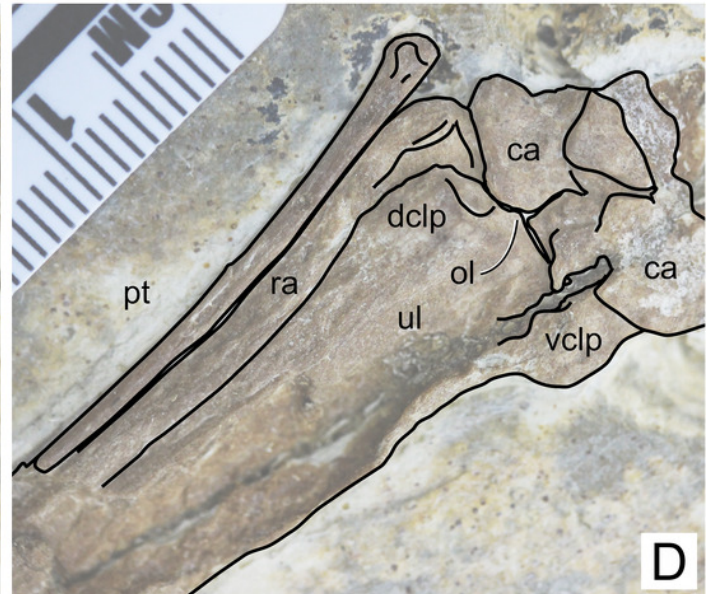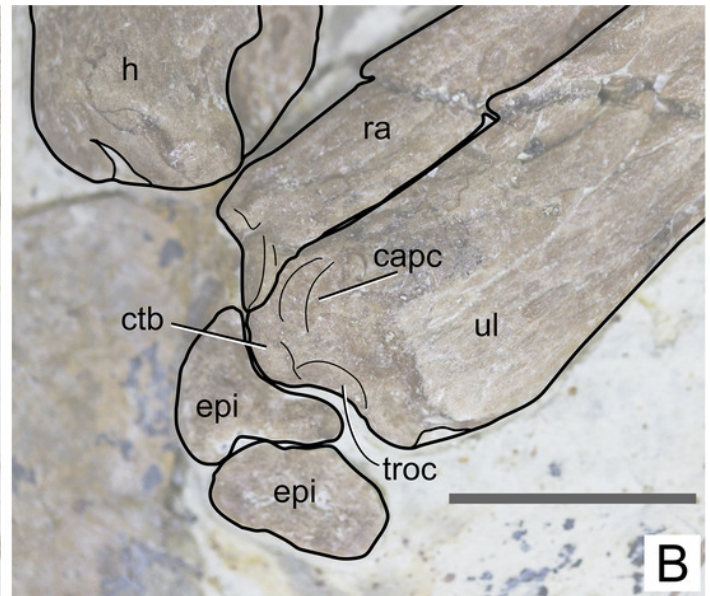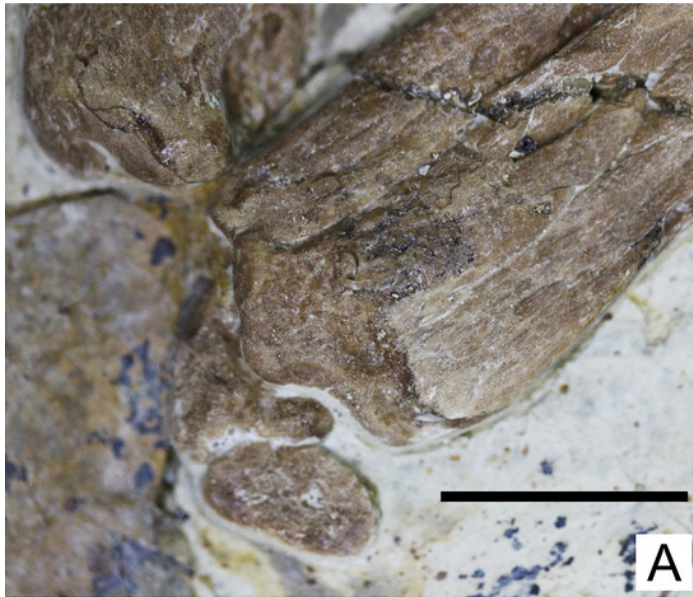
Figure 6

Figure 6. Specimen D3072, right carpus and manus.

(A) Photograph and (B) schematic drawing. Abbreviations: d, digit; dc, distal carpals; etp, extensor tendon process; lpc, lateral proximal carpal; mc, metacarpal; mpc, medial proximal carpal; pt, pteroid; ra, radius; ul, ulna; pc, preaxial carpal; pf, pneumatic foramen; ph, phanlanx; pt, pteroid. Scale bar equals 10 mm.
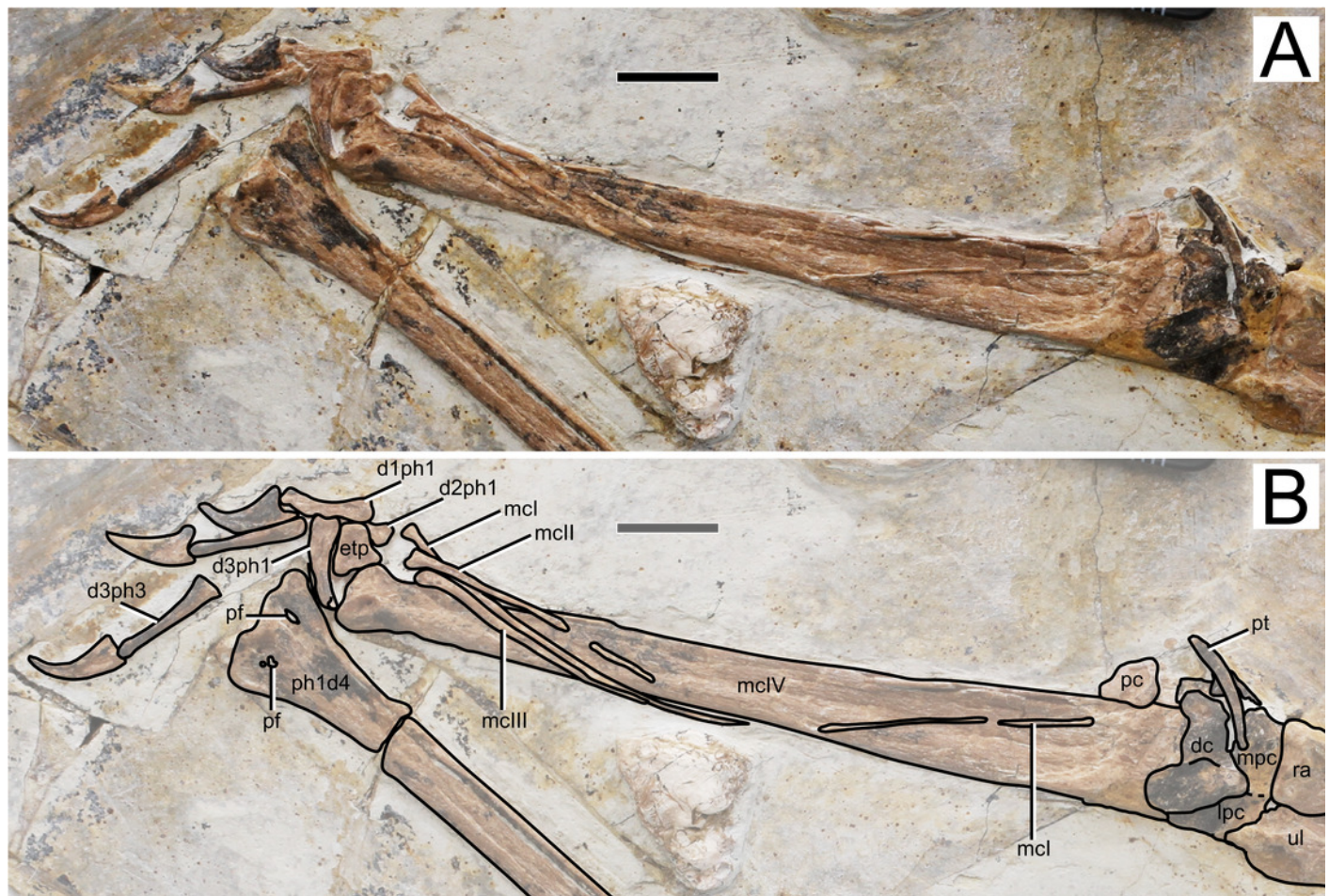
Figure 7

Figure 7. Specimen D3072, pedes.

Right pes, (A) photograph and (B) schematic drawing. Left pes, (C) photograph and (D) schematic drawing. Abbreviations: f, fibula; ldt, lateral distal tarsal; lpt, lateral proximal tarsal; mdt, medial distal tarsal; mt, metatarsal; t, tibia; us, ungual sheath. Scale bar equals 10 mm.
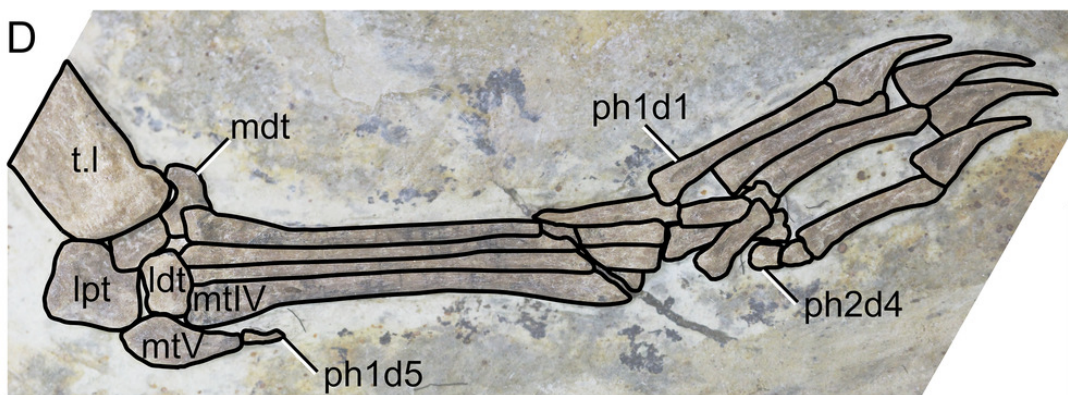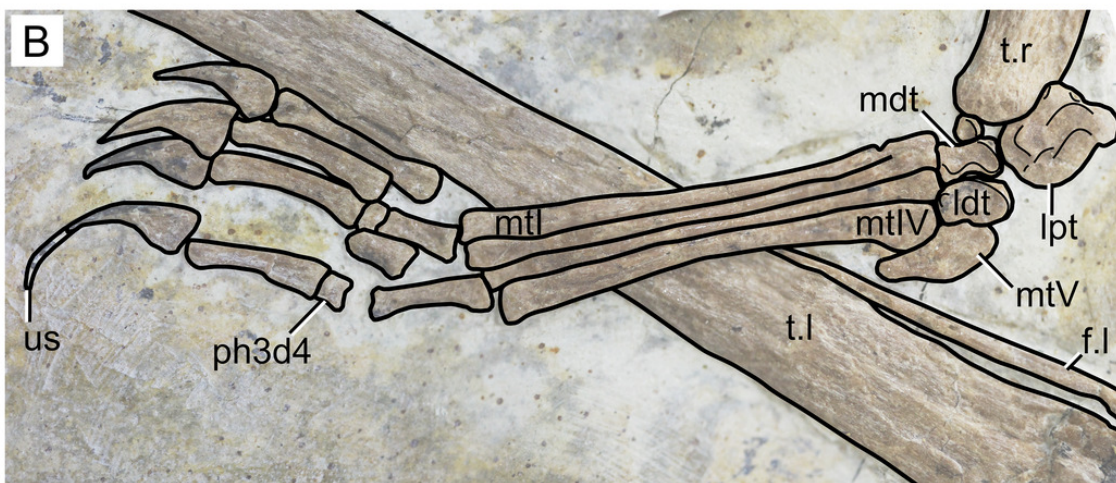
Figure 8

Figure 8. Wing elements proportions (in percentage of total wing length) in selected azhdarchoids.

Data source: *Sinopterus dongi* (holotype, IVPP V 13363; Wang & Zhou (2003a); *Sinopterus "jii"* (holotype, GMN-03-11-001; Lü & Yuan, 2005); *S. atavismus* (holotype, XHPM 1009; Lü *et al.*, 2016); *Eopteranodon lii* (D2526, Lü *et al.*, 2006b); D2525 (Lü *et al.*, 2006c); *"Huaxiapterus" benxiensis* (holotype, BXGM V0011; Lü *et al.*, 2007); *"Huaxiapterus" corollatus* (holotype, ZMNH M8131), Lü *et al.* (2006a); *Tupandactylus navigans* (GP/2E 9266), Beccari *et al.* (2021); *Caiuajara dobruskii* (composite), Manzig *et al.* (2014); *Jidapterus edentus* (holotype, RCPS-030366CY), Wu *et al.* (2017); *Chaoyangopterus zhangi* (holotype, IVPP V 13397), Wang & Zhou (2003b); *Shenzhoupterus chaoyangensis* (holotype, HGM 41HIII-305A), Lü *et al.* (2008). Abbreviations: d, digit; hol., holotype; McIV, metacarpal IV; ph, phalanx.
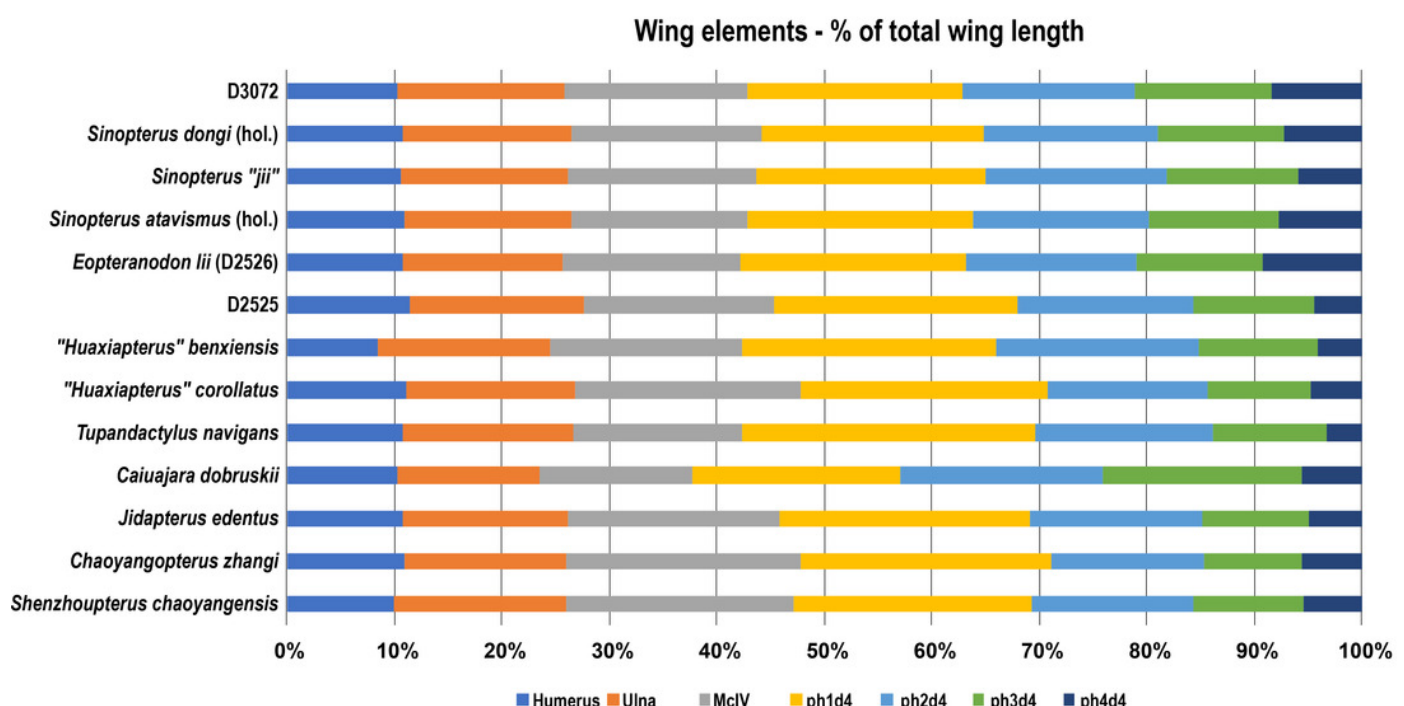
Figure 9

Figure 9. Humerus morphology in tapejarines.

(A) *Caupedactylus ybaka*, right humerus in anterior view, drawn from Kellner (2013). (B) D3072, left humerus in an approximately ventral view. (C) *Tupandactylus navigans*, mirrored right humerus in posterior view, drawn from Beccari *et al.* (2021). (D) *Caiuajara dobruskii*, mirrored left humerus in anterior view, drawn from Manzig *et al.* (2014). (E) *Tapejara wellnhoferi*, right humerus in anterior view, drawn from Eck *et al.* (2011). Notice the variation in the orientation of the deltopectoral crest, perpendicular to humeral shaft in (A) and (B), and oblique in (C), (D) and (E). Scale bars equal 10 mm.
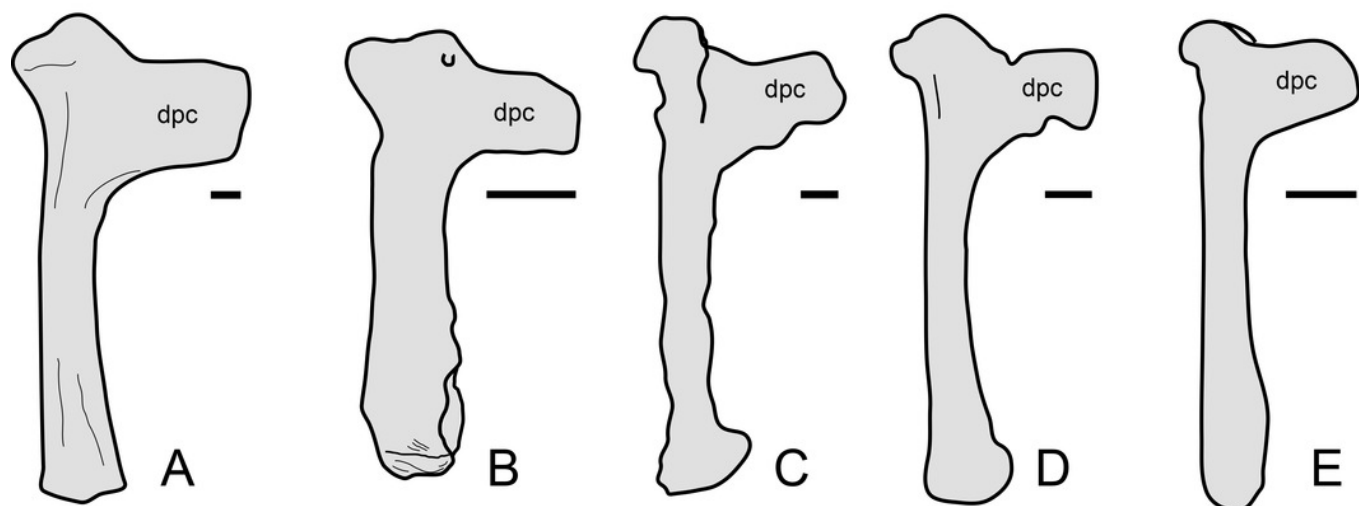
Table 1. Measurements of limb elements in the new specimen D3072.

Elements	length	width
Cervicals 3-7	12.4/22.5/19.0/17.4/15.5	8.3/9.1/9.6/8.6/10.2 (height)
Dorsal series	66.7 (preserved)	?
Coracoid	32.8 (preserved)	5 (shaft)
Humerus (l.)	55.1	9.1 (shaft)
Deltopectoral crest (l.)	14.1	10.5
Ulna/radius (l.)	82.6/82.6	8.2/?
Pteroid (l.)	32.0 (preserved)	-
Metacarpals I-III (r.)	88.5/34.2/33.3	~1 (midshaft)
Metacarpal IV (r.)	90.8	8.6
Manual digit 1 (r.), phalanges 1 – 2	11.8/12.5	~2 (midshaft)/5.1 (dorsoventral)
Manual digit 2 (r.), phalanges 1 – 3	?/14.9/11.3	?/~2 (midshaft)/5 (dorsoventral)
Manual digit 3 (r.), phalanges 1 – 4	22.0/?/14.5/12.1	~1.5 (midshaft)/?/~1.5 (midshaft)/4.6 (dorsoventral)
Wing phalanx 1	107.7 (r.), 108.6 (l.)	5.8 (r.), 5.9 (l.)
Wing phalanx 2	85.6 (r.)	4.1 (r.), 4.2 (l.)
Wing phalanx 3	67.8 (r.)	2.2 (r.), 2.3 (l.)

Wing phalanx 4	45.0 (r.), 46.5 (l.)	1.8 (r.), 1.9 (l.)
Tibia (r.)	97.7	8.58 (shaft)
Metatarsals I-IV	23.7/23.0/22.6/21.5 (l.)	1.0/0.8/0.7/1.2 (r.)
	24.9/23.6/23.1/22.1 (r.)	1.1/0.9/0.8/1.2 (l.)

4 **Table 1. Measurements of the new specimen D3072.** Measurements given in milimeters.